

THE MASS OF THE GLOBULAR CLUSTER NGC 6388

GARTH ILLINGWORTH AND K. C. FREEMAN

Mount Stromlo and Siding Spring Observatory, Research School of Physical Sciences, Australian National University

Received 1973 December 26

ABSTRACT

The central velocity dispersion has been derived for the globular cluster NGC 6388 from high-dispersion coude spectra of the integrated light. A new method using Fourier techniques for accurately determining the velocity dispersion from integrated light spectra is described. The mass was obtained from King's models, using photoelectric surface photometry and star counts to define the surface density distribution. The resulting mass is $(1.3 \pm 0.3) \times 10^6 M_{\odot}$, and the mass-luminosity ratio $(M/L_{\nu}) = 1.7 \pm 0.4$ solar units.

Subject heading: globular clusters

I. INTRODUCTION

The masses of globular clusters are very poorly known. Direct dynamical mass estimates are available only for M92 (Wilson and Coffeen 1954; Schwarzschild and Bernstein 1955), ω Centauri (Dickens and Woolley 1967), and 47 Tucanae (Feast and Thackeray 1960). These are based on the velocity dispersion derived from radial-velocity measurements for individual stars and are therefore fairly uncertain. Masses can also be estimated from the luminosity function, as for M3 (Sandage 1957): these depend on assumptions about the luminosity function for stars fainter than the observational limit, and so again are rather uncertain.

The purpose of this *Letter* is to present the first results of a new set of dynamical mass estimates for globular clusters, in which the velocity dispersion at the center of the cluster is measured from high-dispersion spectra of the integrated light. We felt that the result for NGC 6388 was interesting enough to present here before the main body of the mass program was complete. A description is also given of a new and powerful procedure for deriving the velocity dispersion of a stellar system from the spectrum of its integrated light.

II. THE VELOCITY DISPERSION

NGC 6388 is a concentrated, metal-rich globular cluster with a high central surface brightness: this makes it an ideal object for high-dispersion spectroscopy. Spectra of the cluster and a range of comparison stars were obtained with the coude spectrograph of the 188-cm reflector, using a Carnegie two-stage image intensifier. The spectral region was 5150–5300 Å, and the dispersion was 6.7 Å mm^{-1} . The instrumental profile has a half-width of 0.5 Å , which is due almost entirely to the image tube.

The star selected as being more closely similar overall in its line strengths to the cluster was HD 37160 (G8 III, $[\text{Fe}/\text{H}] \sim -0.7$), a giant in the σ Puppis group (Eggen 1971). All spectra were measured on the same digital microphotometer.

We used two procedures for estimating the velocity dispersion. The first is the traditional method (e.g., Richstone and Sargent 1972): the stars contributing to the integrated light have an assumed Maxwellian velocity distribution, and numerical evaluation of the integral

$$S(\lambda_0) = \frac{c}{\lambda_0 (2\pi \langle v^2 \rangle)^{1/2}} \times \int_{-\infty}^{\infty} I(\lambda) \exp \left[\frac{-c^2 (\lambda - \lambda_0)^2}{2 \langle v^2 \rangle \lambda_0^2} \right] d\lambda \quad (1)$$

gives the broadened star spectrum $S(\lambda_0)$ for comparison with the observed cluster spectrum. Here $I(\lambda)$ is the observed star spectrum. The best-fit $S(\lambda_0)$ chosen is shown in figure 1, for a velocity dispersion $\langle v^2 \rangle^{1/2} = 19 \text{ km/sec}$. The standard error of $\langle v^2 \rangle^{1/2}$, estimated from figure 1, is about 4 km s^{-1} . The major difficulty in this procedure is obtaining a local fit of $S(\lambda_0)$ to a large number of lines in the composite cluster spectrum.

As an aid to fitting $S(\lambda_0)$ to the cluster spectrum, the cluster spectra were filtered to remove the high-frequency noise component (cf. Morton and Chevalier 1972), as described by Brault and White (1971). An FFT algorithm gave the Fourier transform of the cluster spectra; the filter

$$\begin{aligned} \Phi &= 1, & \nu &\leq \nu_1, \\ &= \frac{1}{2} \left[1 - \cos \frac{\pi(\nu_2 - \nu)}{\nu_2 - \nu_1} \right], & \nu_1 &< \nu < \nu_2, \\ &= 0, & \nu &\geq \nu_2, \end{aligned} \quad (2)$$

was applied; and the filtered spectra were derived by the inverse transform. The frequencies ν_1 , ν_2 were carefully chosen so that no distortion occurred when a well-exposed star spectrum was filtered in this way. Further care was taken to ensure that the transform was reliable, by minimizing aliasing and leakage using methods outlined by Brault and White. The filtering procedure made the fitting of $S(\lambda_0)$ to the cluster spectrum much easier.

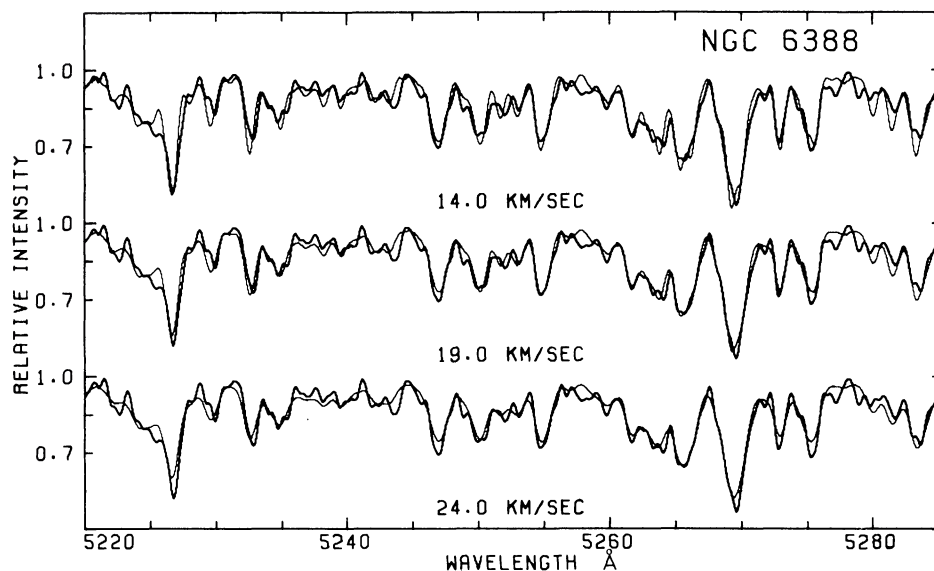


FIG. 1.—The cluster spectrum (*wide lines*) is fitted with the broadened spectrum of HD 37160 (*narrow lines*) for three velocity dispersions given beneath each spectrum. The continuum levels are normalized to 1.0. The spectra have been noise filtered as described in the text.

Our second procedure is based on comparison of the power spectra of the cluster spectrum and a star spectrum of similar (but not necessarily locally identical) line strengths: this gives the velocity dispersion quickly and accurately. Assuming that $\lambda_0^2 \langle v^2 \rangle$ in the integral of equation (1) is constant over the small wavelength region involved (the change in $\lambda_0^2 \langle v^2 \rangle^{1/2}$ over this region is only of order $\pm 1.5\%$, which is negligible), then the integral is a convolution integral. If we write this convolution as $S(\lambda) = I(\lambda) * G(\lambda)$, then it follows from the convolution theorem that $S^*(\nu) = I^*(\nu)G^*(\nu)$, where the asterisk denotes the Fourier transform. The Gaussian function $G(\lambda)$ transforms to $G^*(\nu)$, a real function, in this way:

$$\frac{c}{\lambda_0} (2\pi \langle v^2 \rangle)^{-1/2} \exp\left(-\frac{c^2 \lambda^2}{2\lambda_0^2 \langle v^2 \rangle}\right) \rightarrow \exp(-2\pi^2 \lambda_0^2 \langle v^2 \rangle \nu^2 / c^2). \quad (3)$$

The power spectrum

$$P(\nu) = S_{\text{Re}}^2(\nu) + S_{\text{Im}}^2(\nu) = G^{*2}(\nu)[I_{\text{Re}}^2(\nu) + I_{\text{Im}}^2(\nu)] \quad (4)$$

was calculated for a range of values of $\langle v^2 \rangle$, as plotted in figure 2*a*. Comparison of the slopes of the convolved star power spectrum of equation (4) with the cluster power spectrum then gives the velocity dispersion; see figure 2*b*. The selection of a star with similar line strengths ensures that the *intrinsic* cluster spectrum and the star chosen have similar slopes, so that the observed cluster $P(\nu)$ can be validly matched. Two procedures were used to improve the accuracy of the

velocity dispersion determination from the power spectra of figs. 2*a* and 2*b*. (1) A running mean over ± 0.06 cycle \AA^{-1} has been applied to the $P(\nu)$ to reduce the large-amplitude fluctuations inherent in transforms of spectral regions containing many lines. (2) The mean noise level has been removed since, relative to the signal power, this level is different for the star and cluster power spectra. The mean slopes of the noise power spectra from several calibration plates were found to be closely the same. The normalized mean noise level was then removed from the power spectra of figures 2*a* and 2*b*; the level is shown by the dotted lines.

In summary, the procedure involves these four steps: (1) digitizing the cluster and comparison-star spectra; (2) taking the Fourier transform of both, ensuring that aliasing and leakage are minimized; (3) multiplication of the star transform with the exponential of equation (3), using appropriate parameters; (4) comparison of the resulting star $P(\nu)$ with the cluster $P(\nu)$.

From figure 2 we adopt $\langle v^2 \rangle^{1/2} = 19 \text{ km s}^{-1}$. The standard error of $\langle v^2 \rangle^{1/2}$, estimated from figure 2, is only about 1 km s^{-1} . This procedure is obviously much more accurate than the conventional method illustrated in figure 1.

III. THE SURFACE DENSITY DISTRIBUTION

We will use King's (1966*a*) models to estimate the cluster mass. These models should give a more reliable mass than that given by straightforward application of the virial theorem (see § IV). The surface density distributions for these models have two length scales, the core radius r_c and the tidal cutoff radius r_t . Photo-

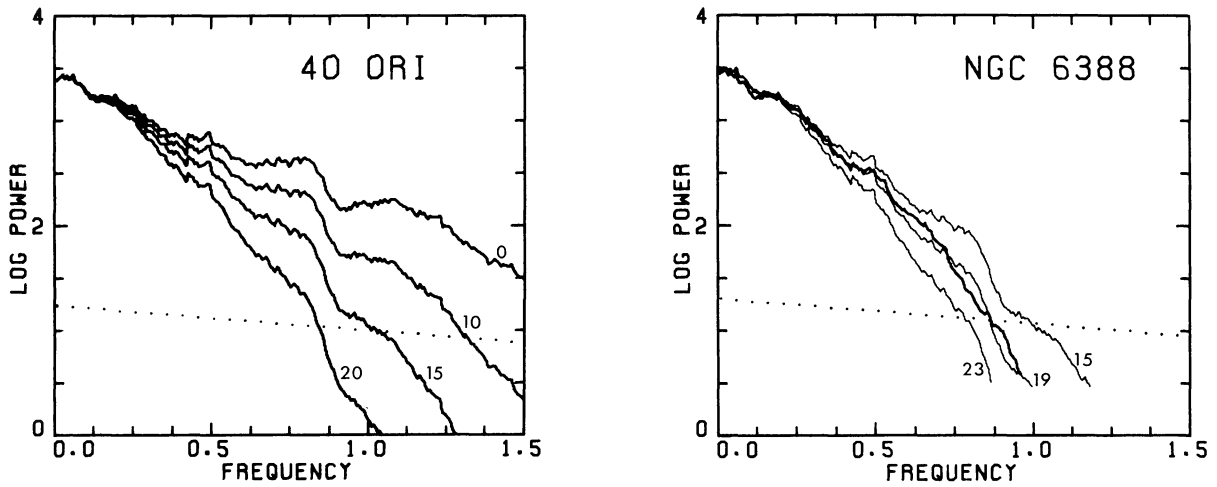


FIG. 2.—(a) Smoothed power spectra for the comparison star 40 Ori (HD 37160) convolved with a range of velocity dispersions (in km s⁻¹: indicated in figure). The mean noise level is indicated by the dotted line. (b) The cluster power spectrum (*wide line*) is fitted by the power spectra for 40 Ori convolved with the velocity dispersions indicated on the figure. The frequency scale is cycles per Å. The cluster mean noise level is indicated by the dotted line.

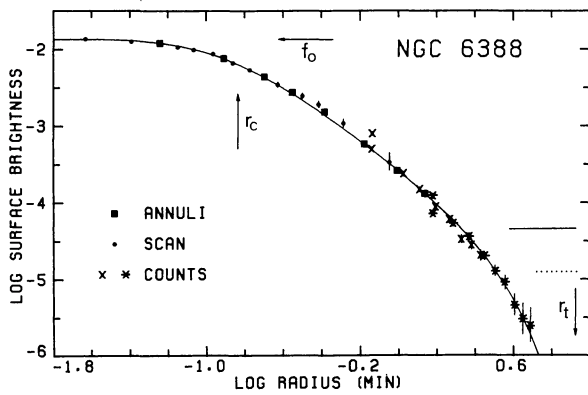


FIG. 3.—The observed surface density distribution from surface photometry and star counts fitted by a King theoretical distribution with $\log(r_t/r_c) = 1.75$. The central brightness f_0 , core radius r_c , and tidal cutoff r_t are indicated. The unit of surface brightness is $V = 10.00$ mag per (arc sec)². The mean sky brightness (*continuous line*) and the background for the star counts (*dotted line*) are shown.

measured at equal intervals in radius from the cluster center; these measures are shown in figure 3, after applying corrections to compensate for the smoothing due to the finite aperture size. We have also used star counts, from two visual photographs taken with the 100-cm reflector, to delineate the tidal radius and to check the choice of the concentration ratio r_t/r_c . The error bars on the plotted points are sampling errors calculated as described by King (1966b) and King *et al.* (1968) for the surface photometry and star counts, respectively.

The distance modulus and reddening have been derived from fitting a preliminary color-magnitude diagram of NGC 6388 (Freeman and Ford, unpublished) to other metal-rich cluster C-M diagrams collected by White (1970).

The adopted parameters for NGC 6388 are collected in table 1. The total apparent magnitude comes from integrating the luminosity profile of figure 3 out to the tidal radius.

electric surface photometry, by two different methods over the inner 1.5 in radius, was used to measure r_c . (1) Observations in the V-band, using apertures from 9" to 3' diameter centered on the cluster nucleus, gave the mean surface brightness at eight different radii: surface brightnesses derived by differencing the successive aperture measures were assigned to the radii which bisect the area of the resulting annuli (see annuli, fig. 3). Mean-to-local corrections, which never exceeded 7 percent, were applied as detailed by King (1966b). (2) To confirm these primary measures, a scan was obtained through a 14" aperture (V-band again) by drifting the telescope slowly across the cluster. From the chart record, the surface brightness has been

TABLE 1
OBSERVED PARAMETERS

$\langle v^2 \rangle^{1/2}_{\text{obs}}$ (km s ⁻¹)	19.0
$\langle v^2 \rangle^{1/2}_c$ (km s ⁻¹)	19.7
$\log(r_t/r_c)$	1.75
r_t (pc)	33.4
r_c (pc)	0.59
μ	34.8
$(m - M)_0$	15.7 ± 0.4
Distance (kpc)	13.8 ± 2.7
$E(B - V)$	0.38
m_V	6.83
M_V	-10.0 ± 0.4
$(B - V)_0$	0.79

IV. THE MASS

From equations (15) and (40) of King's (1966a) paper the cluster mass is given by

$$M = 9r_c \mu \langle v^2 \rangle_c / 4\pi G, \quad (5)$$

where μ is a tabulated function of the ratio (r_t/r_c) and $\langle v^2 \rangle_c$ is the line-of-sight component of the *central* velocity dispersion. This is slightly greater (see table 1) than the *observed* velocity dispersion due to contributions to the spectra from noncentral regions where the velocity dispersion is less. Using the parameters derived in §§ II and III (tabulated in table 1), we calculate $M = (1.3 \pm 0.3) \times 10^6 M_\odot$ and $(M/L_V)_\odot = 1.7 \pm 0.4$. The standard errors are formal. They do not include possible errors resulting from differences between the mass and light distributions and from the use of a single-mass model. Table 2 summarizes some parameters derived from the model using the data given in table 1: Ω , ρ_0 , and v_{es} are the total potential energy of the cluster, the central density, and the central escape velocity, respectively.

We should comment here on the advantage of using self-consistent models to estimate the mass. The conventional procedure is to use the virial theorem with

TABLE 2
DERIVED PARAMETERS

Mass ($10^6 M_\odot$)	$(M/L_V)_\odot$	$(M/L_B)_\odot$	ρ_0 ($M_\odot \text{ pc}^{-3}$)	Ω (ergs)	v_{es} (km s^{-1})
1.3 ± 0.3	1.7 ± 0.4	1.9	1.8×10^5	1.8×10^{52}	77

the assumption that the velocity dispersion is constant throughout the system. This can lead to significant errors. For example, say we calculate Ω from the appropriate King model and then apply the virial theorem in the usual way; we then overestimate the mass by 70 percent because we have not included the decrease of velocity dispersion with radius that is a feature of the self-consistent models.

V. COMMENTS

Mass estimates from the work of the authors mentioned in § I give $M/L \sim 1$ for globular clusters. This value is supported by the more accurate result obtained here.

Typical globular-cluster luminosity functions (i.e., M3 [Sandage 1957], or M5 [Simoda and Tanikawa 1972]) combined with the Weilen (1973) solar-neighborhood function for the unobservable low-mass stars give $(M/L_V)_\odot = 1.1$ and 1.5 for M3 and M5, respectively. The agreement here between the dynamical and luminosity-function M/L estimates is good. Further work needs to be done to improve the dynamical mass estimate by using many-mass models (e.g., see Prata 1971a, b) and to improve the luminosity functions by compensating for the distribution differences for stars of different masses (see King and Wilson 1972). Then elucidation of the degree of low-mass star loss due to the dynamical evolution of the cluster and of the present form of the mass function should be possible.

We would like to thank Dr. A. J. Kalnajs for suggestions which led to the Fourier method used here. Garth Illingworth is grateful for the financial support of an Australian National University Research Scholarship.

REFERENCES

- Brault, J. W., and White, O. R. 1971, *Astr. and Ap.*, **13**, 169.
 Dickens, R. J., and Woolley, R. 1967, *R.O.B.*, No. 128.
 Eggen, O. J. 1971, *Pub. A.S.P.*, **83**, 251.
 Feast, M. W., and Thackeray, A. D. 1960, *M.N.R.A.S.*, **120**, 463.
 King, I. R. 1966a, *A.J.*, **71**, 64.
 ———. 1966b, *ibid.*, p. 276.
 King, I. R., Hedemann, E., Hodge, S. M., and White, R. E. 1968, *A.J.*, **73**, 456.
 King, I. R., and Wilson, C. P. 1972, *Dudley Obs. Reports*, ed. A. G. D. Philip, No. 4, p. 29.
 Morton, D. C., and Chevalier, R. A. 1972, *Ap. J.*, **174**, 489.
 Prata, S. W. 1971a, *A.J.*, **76**, 1017.
 ———. 1971b, *ibid.*, p. 1029.
 Richstone, D., and Sargent, W. L. W. 1972, *Ap. J.*, **176**, 91.
 Sandage, A. 1957, *Ap. J.*, **125**, 422.
 Schwarzschild, M., and Bernstein, S. 1955, *Ap. J.*, **122**, 200.
 Simoda, M., and Tanikawa, K. 1972, *Pub. Astr. Soc. Japan*, **24**, 1.
 Weilen, R. 1973, paper presented to IAU General Assembly, Sydney.
 White, R. E. 1970, *Ap. J. Suppl.*, **19**, 343.
 Wilson, O. C., and Coffeen, M. F. 1954, *Ap. J.*, **119**, 197.